CURRENT-VOLTAGE BEHAVIOR IN LIQUID-STATE ORGANIC FIELD-EFFECT TRANSISTORS (LOFETS)

CURRENT-VOLTAGE BEHAVIOR IN LIQUID-STATE ORGANIC FIELD-EFFECT TRANSISTORS (LOFETS)

By

Feihong Nan, B. Eng.

A thesis

Submitted to the School of Graduate Studies

in Partial Fulfillment of the Requirements

For the Degree

Master of Applied Science

McMaster University

MASTER OF APPLIED SCIENCE (2008) McMaster University

(Materials Science & Engineering) Hamilton, Ontario

TITLE: Current-voltage behaviour in Liquid-state organic field-effect transistors (LOFETs)

AUTHOR: Feihong Nan, B. Eng., (Kunming University of Science and Technology, China)

SUPERVISOR: Dr. Gu Xu

NUMBER OF PAGES: XIII, 65

ABSTRACT

In this thesis, the current-voltage (I-V) behaviour of Liquid Organic Field-Effect Transistor (LOFET) was systematically studied with respect to the gate voltage, channel length and channel fluid. LOFETs in both internal and external gate modes were successfully fabricated in four-probe configuration.

It was discovered that the effect of gate voltage on the source-to-drain current of LOFETs was significant. The drain current clearly increased when the gate voltage increased. This phenomenon was found in all LOFETs samples with different channel fluids and channel lengths. In addition, it was also proved that anions are the majority carriers in LOFETs. The concentration of anions inside the LOFET channel increased while applying a larger voltage to the gate, resulted in an increase of the drain current. This achievable gate modulation set up a solid foundation for further research on the manipulation of ionic and molecular species.

It was also obtained that the drain current was changed with variable channel lengths. The current through the LOFET channel decreased while the channel length increased. At the same time, the difference between drain current in various channels evidently increased when the gate voltage increased from 0 to 5V. This was found to be due to the anion concentration change with varying gate voltages.

The drain currents through LOFET channels filled with fluids of different polarities were also measured. It was observed that when the polarity of the

molecule increased from that of 4,4'-Dihydroxybiphenyl to that of 2-Amino-4 Phenylphenol, the drain current increased significantly. At the same time, the difference between drain current in specific solutions was also more significant, when applying higher voltage to the gate. Combining these results with the gate modulation above, there is great potential of developing new sensing techniques and even logic operation in the future.

This work represents a step towards a new group of cheap and effiecient electronic components of LOFETs. Guided by systemic observations from the effects of gate voltage, channel length and fluid structure, there is no doubt that LOFET will become a more attractive research topic because of its promising advantages, such as easy fabrication, low cost and its highly sensitive response.

ACKNOWLEGEMENTS

The author wishes to be deeply grateful to her supervisor, Dr. Gu Xu, for his great patience and instructive supervision throughout the thesis work.

The author would like to thank Dr. Jiachun Deng for his helpful discussion and advice.

Very special thanks must be given to Jim Garrett, Dr. Jim Britten, Dr. Huazhong Shi and Steve for their invaluable discussion and kind help.

The author would like to thank her group members, Dr. Hualong Pan, Dr. Roy Luo, Dr. Richard Klenkler, and Han Yan, for their helpful advice and assistance with this project.

The author wishes to thank her parents and sister, for their constant support and encouragement.

The financial support from NSERC and McMaster University is greatly appreciated.

TABLE OF CONTENTS

LIST OF FIGURES

1 INTRODUCTION

It is beyond anyone's imagination how fast the Field-Effect Transistors (FETs) industry has been booming over the past several decades. The invention of germanium point-contact transistor by Shockley and his two Bell Labs colleagues, Brattain and Bardeen, not only brought them the Nobel Prize in Physics in 1956, but also formed a milestone in the 20th century electronic industry. In addition, Metal-Oxide-Semiconductor FETs (MOSFETs) and Complementary MOSFETs developed respectively by Kahng and Wanlass in the 1960's greatly motivated the IFET to dominate the semiconductor industry for their wide range of applications from memories and microprocessors to signal and imaging systems [1, 2].

Since the 1980's, Organic Field-Effect Transistors (OFETs) based on conjugated polymers, oligomers, or other organic molecules have been envisioned as obvious alternative to traditional IFETs for their structured flexibility, low-temperature fabrication and low cost. In this case, OFETs hold promise for applications in large-area, flexible and ultralow-cost electronics such as computer displays and disposable cell phones [3-5].

During the last decade, interest in microfluidic circuitry has grown steadily with the advent of advanced etching and lithography techniques capable of creating fluidic circuits. This became a driving force for the development of M/NFET for applications in biomedical research, environmental testing and medical diagnostics [6-10].

It is obvious that the trend in the FET industry is always directing to exploit the modest end of cost and performance. That is why materials scientists and device engineers have been collaborating to develop new breeds of cheap and efficient electronic components. In current LOFET research, the device is simply assembled with micro-glass slides and metal electrodes. Current flow between source and drain is impacted by the gate voltage. I-V behaviours corresponding to different gate voltages, channel lengths and fluid types, predict the potential advantages of LOFETs of easy fabrication, low cost and sensitive response, applying in biochemical testing techniques in the future.

In this thesis, after detailed review of history, working mechanism, advantages and applications of existing IFETs, OFETs, and M/NFETs, the limitations in the current device, which is also the motivation of the study on LOFETs, will be summarized. The experimental set-up, testing technique and results, followed by the discussion and future work, will be given in separate chapters.

2 LITERATURE REVIEW

2.1 History of Field-Effect Transistors

2.1.1 History of Inorganic Field-Effect Transistors

The Field Effect Transistor was first filed as a patent by Julius E. Lilienfeld in 1926, "Method and Apparatus for Controlling Electric Currents," in which a three-electrode structure using copper-sulfide semiconductor material was proposed. However, he never got the device to work because he did not fully appreciate the role of surface defects or surface states [11-13].

In the process of trying to experimentally demonstrate such a field-effect transistor, Bardeen, Brattain and Shockley invented the bipolar transistor, the world's first transistor, at the Bell Telephone Laboratories in 1947. This germanium point-contact device, along with its field-effect counterpart, reigned supreme in the early days of semiconductor integrated electronics [14-17].

It was only much later, after the problem of the surface states was resolved by growing an oxide insulator on Si, that the first MOSFET was demonstrated in 1960 by Kahng and Atalla, which had been long anticipated by Lilienfeld, Heil, Shockley and others. Unlike previously bipolar transistors, the various types of MOSFETs are characterized by high input impedance, since the control voltage is applied to a reverse-voltageed junction or Schottky barrier, or across an insulator. These devices are particularly well suited for controlled switching between a

conducting state and a nonconducting state, and are therefore useful in digital circuits. They are also suitable for integration of many devices on single chips. In fact, millions of MOS transistors are commonly used together in semiconductor memory devices and microprocessors today[17-21].

2.1.2 History of Organic Field-Effect Transistors

Organic semiconductors were identified as early as 1948 [22]. However, in spite of several significant advances, such as electroluminescence and photovoltaic effect, these materials remained confidential for several years [23-26]. The first organic field-effect transistor was reported until 1986, with device made on an electrochemically grown polythiophene film. Different from geometry of the MOSFETs, OFETs used "thin film" transistor (TFT) architecture, in which the organic semiconducting film worked as an active layer for charge transport [27-29]. Over the last decades, the improving performance of OFETs made it possible to develop low-cost, large-area plastic electronics by a number of industrial laboratories. As noted by Dimitrakopoulos and Malenfant in their 2002 review, industrial emphasis is shifting away from organic semiconductor testing and more towards manufacturing process development [30, 31].

2.1.3 History of Micro/Nanofluidic Field-Effect Transistors

Interest in micro/nanofluidic technique has grown steadily over the past decade [6-34]. The first commercial Microfluidic "lab-on-a-chip" system was introduced for life science applications in 2003 [35]. Following that, several lab-on-a-chip companies, including Aclara, Caliper, and Orchid Biosciences, have developed micro/nanofluidic technologies that work for highly predictable and homogeneous samples that are common in the drug discovery process, whether in compound screening, genomic analysis, or proteomics [36-38].Later in 2005, the control of current flow in a liquid-state field-effect transistor was achieved by using electrowetting [10], an important enabling technology in microfluidics [39, 40]. In the same year, nanofluidic FET was reported which exhibited rapid field effect modulation of ionic conductance [8].

2.2 Working Mechanisms of Field-Effect Transistors

2.2.1 Working Mechanism of Inorganic Field-Effect Transistors

Although FETs can be built according to several architectures, the MOSFET structure, whose parent structure was established in 1960 by Kahng [18, 29], is one of the most widely used inorganic field-effect transistors in digital integrated circuits. Channel current in MOSFET is controlled by a voltage applied at a gate electrode which is isolated from the channel by an insulator. Such devices are

made by using metal or heavily doped polysilicon for the gate electrode, SiO_2 for the insulator, and silicon for the semiconductor The term of Metal-Oxide-Semiconductor Field-Effect Transistor (MOSFET) is commonly used [13].

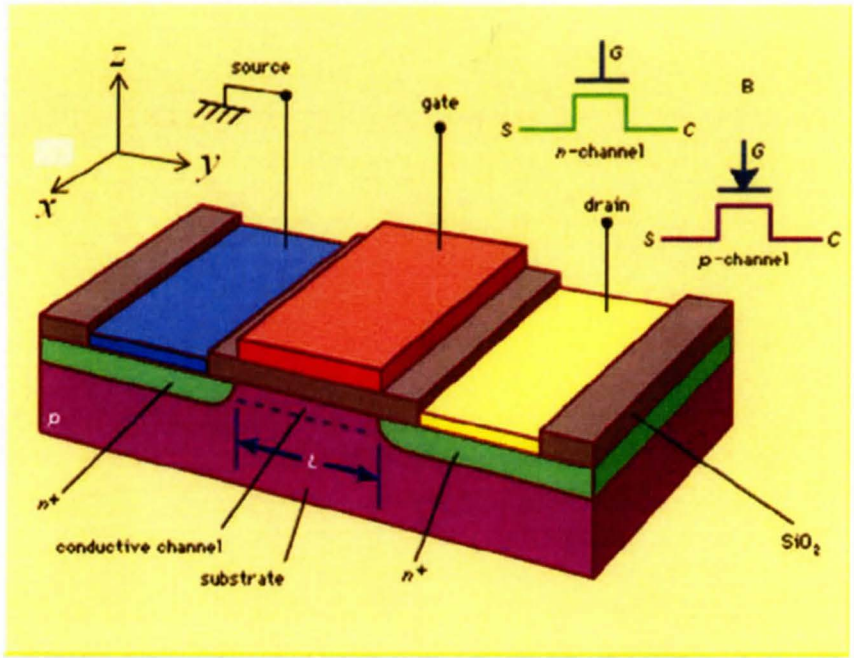

Figure 2- 1 Tridimensional image of an Enhancement-type n-channel MOSFET, reprinted from Encyclopaedia Britannica, Inc.

Structure

Figure 2- 1 illustrates the basic MOSFET structure for the case of an enhancement-mode n-channel device formed on a p-type Si substrate, where two n+ domains have been diffused; they constitute the source and drain electrodes. A

thin oxide layer separated the conducting gate from the Si substrate. No current flows from drain to source without a conducting n channel between them. This can be clearly understood by looking at the band diagram of the MOSFET in equilibrium along the channel in Figure 2-2. The Fermi level is flat in equilibrium. The conduction band is close to the Fermi level in the n+ source/drain, while the valence band is closer to the Fermi level in the p-type substrate. Hence, there is a potential barrier to the built-in potential of the back to back p-n junctions between the source and drain.

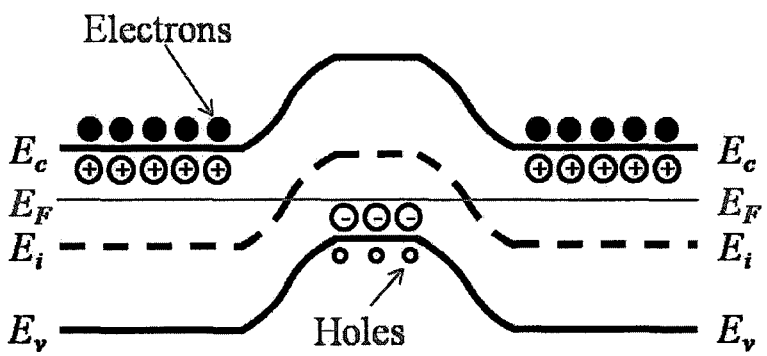

Figure 2-2 Band diagram of the MOSFET in equilibrium along the channel

Gate control operating mode

When a positive voltage is applied to the gate relative to the substrate (which is connected to the source in this case), positive charges are in effect deposited on the gate metal. In response, negative charges are induced in the underlying Si, by the formation of a depletion region and a thin surface region containing mobile

electrons. These induced electrons form the channel of the FET, and allow current flow from drain to source. Since electrons are electrostatically induced in the p-type channel region, the channel becomes less p-type, and therefore the valence band moves down, farther away from the Fermi level. This obviously reduced the barrier for electrons between source, channel, and drain. If the barrier is reduced sufficiently by applying a gate voltage in excess of what is known as the threshold voltage, V_T, there is significant current flow from the source to the drain. For a given value of gate voltage, V_G, there will be some drain voltage, V_D, for which the current becomes saturated, after which it remains essentially constant.

Current-Voltage (I-V) Behaviour

Figure 2-3 and Figure 2-4 illustrated the current-voltage behaviour in inorganic FETs.

Linear region: as the gate voltage increases, more electron charge is induced in the channel and the channel becomes more conducting. The drain current initially increased linearly with the drain voltage.

Pinch off: as drain current flow in the channel keeps increasing, more ohmic voltage drops along the channel such that the channel potential varies from zero near the grounded source to whatever the applied drain potential is near the drain end of the channel. That is, the voltage difference between the gate and the channel reduces from V_G near the source to V_G-V_D near the drain end. Once the

drain voltage is increased to the point that V_G-V_D = V_T, threshold is barely maintained near the drain end, and the channel is said to be pinched off.

Saturation region: increasing the drain voltage beyond the saturated drain voltage $V_{D(sat.)}$ causes the point at which the channel gets pinched off to move more into the channel, closer to the source end. Electrons in the channel are pulled into the pinch-off region and travel at the saturation drift velocity because of the very high longitudinal electric field along the channel. Now, the drain current is said to be in the saturation region because it does not increase with drain voltage significantly.

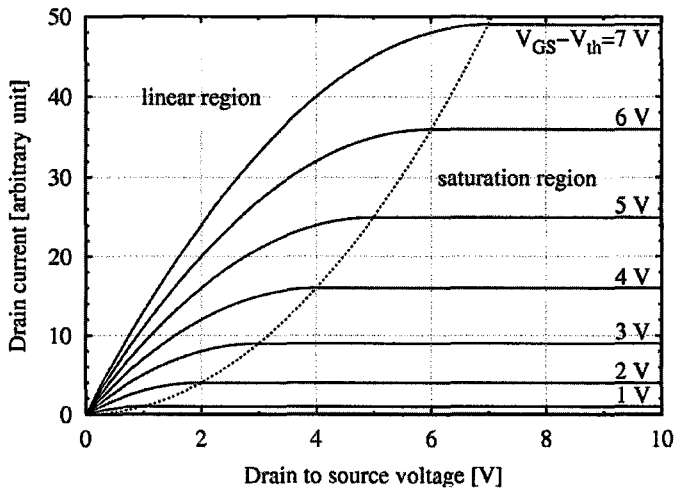

Figure 2-3 MOSFET drain current vs drain-to-source voltage for several values of V_G-V_T, reprinted from Wikimedia Commons

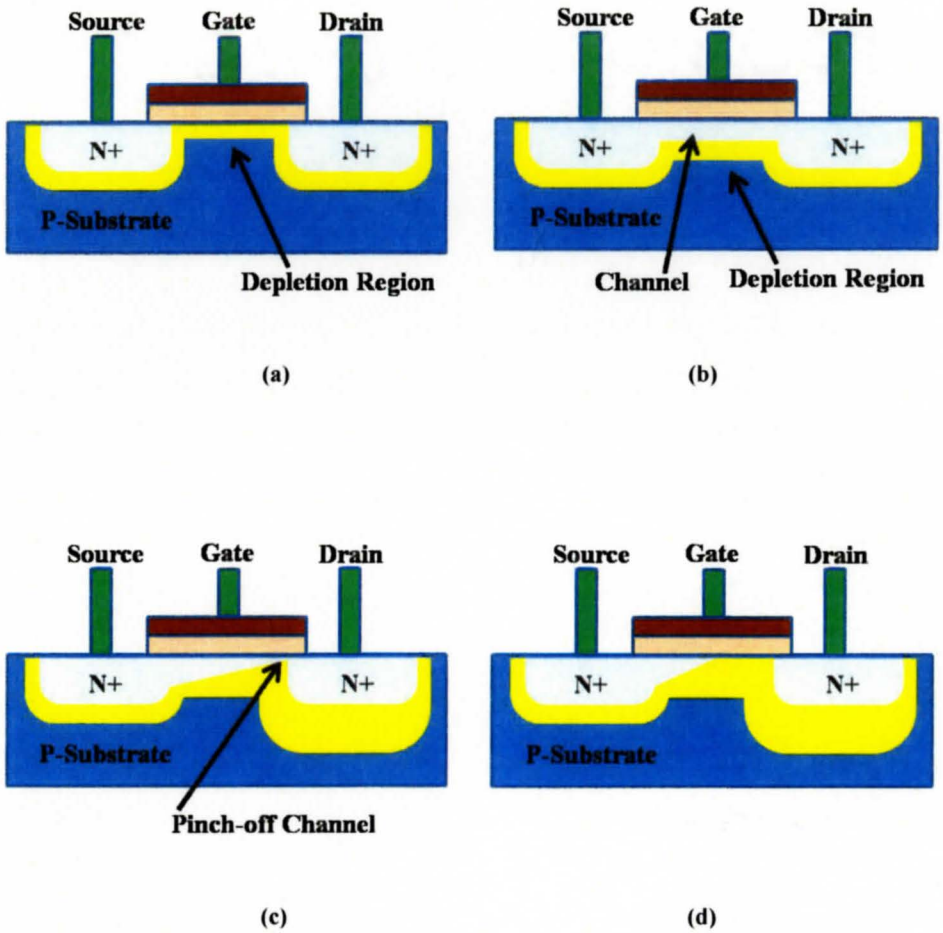

Figure 2-4 MOSFET (a) at equilibrium; (b) linear regime; (c) pinch off; (d) saturation regime

2.2.2 Working Mechanism of Organic Field-Effect Transistors

Similar to Inorganic Field-Effect Transistors (IFETs), Organic Field-Effect Transistors (OFETs) comprise of three electrodes: source, drain and gate shown in Figure 2-5. However, the semiconducting layer of OFETs reduces to a very thin film compared with the bulk solid in IFETs. Secondly, there are no p-n junctions at the source and drain electrodes. Without forming an inversion layer to deliver the mobile charges, the source and drain in OFETs are supposed to easily inject charge into the organic semiconducting layer Thirdly, OFET is n-channelled when the semiconductor type is n-type and p-channelled when the semiconductor is p-type, which is different from the n-type channel formed in p-type substrate in IFETs.

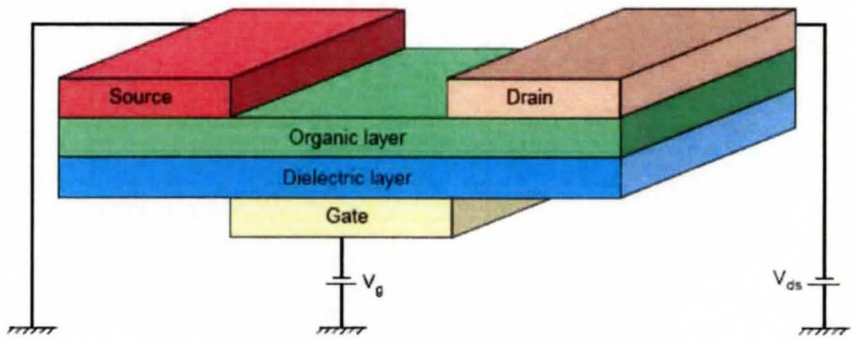

Figure 2-5 Tridimensional image of Organic Filed-Effect Transistor (OFET)

When a gate voltage is applied to the OFET device, a conducting channel is forming at the insulator and semiconductor interface. Most often, the output

characteristics of OFETs have the general shape predicted by Figure 2-3 with well separated linear and saturation regions. Equqations **Error! Reference source not found.** and **Error! Reference source not found.** are widely used to account for these characteristics. [29]

2.2.3 Working Mechanism of Micro/Nanofluidic Field-Effect Transistors

Micro/nanofluidic devices transport ionic or molecular species passively through the channel, analogous to electron transport through source and drain terminals in IFETs. Similar to MOSFETs, introducing field-effect modulation of ionic or molecular species in micro/nanofluidic systems would promote a higher level of controllability and even logic operation.

Microfluidic Field-Effect Transistors

Microfluidic Field-Effect Transistors via electrowetting has similar structure to the conventional solid state MOSFET as shown in Figure 2-6. The device consists of a glass substrate, a dielectric-covered transparent ground electrode, source and drain metal terminals, a hydrophobic insulator layer, a hydrophilic grid (defines circular active device area and confines the oil by strongly attracting water molecules), two fluids (electrolyte KCl and oil), and the top gate electrode.

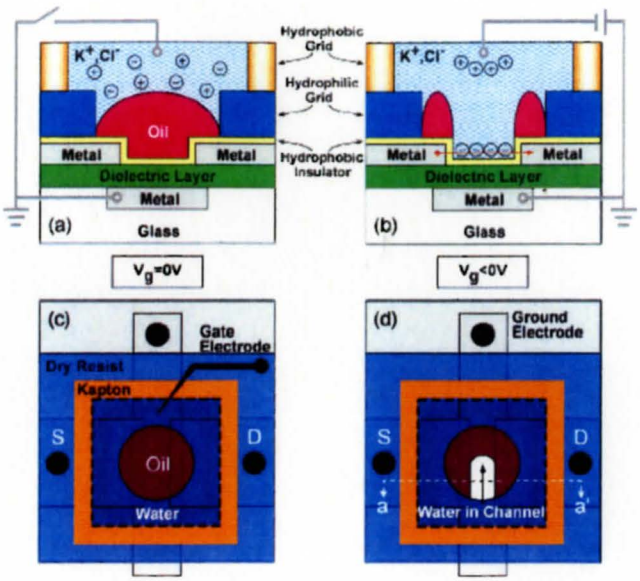

Figure 2-6 Schematic diagram of microfluidic FET via electrowetting, reprinted from ref. 10

For zero gate voltage, the low surface tension oil preferentially covers the low surface energy hydrophobic insulator, forming a thin film that excludes the high surface tension polar electrolyte solution. In this case, the transistor is in the electrically off state, with the source-to-drain channel closed to charge transport.

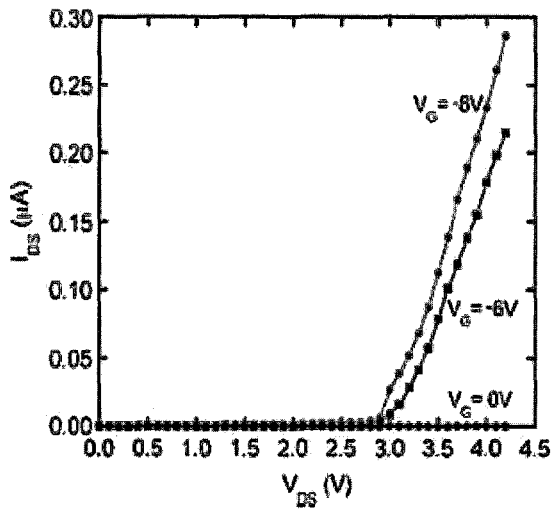

Figure 2-7 Drain current vs drain voltage at different values of gate voltage in Microfluidic FET, reprinted from ref. 10

When a negative voltage is applied to the gate, the electrowetting starts and the resulting field across the hydrophobic insulator effectively increases its surface energy and reduces its hydrophobicity, attracting the polar water molecules and electrolyte anions to the insulator surface and replacing the oil layer. In this case, an electrical channel similar to that is in a MOSFET is formed, through which electrons can flow from source to drain, establishing the Microfluidic FET drain current [10].

Nanofluidic Field-Effect Transistors

The nanofluidic Field-Effect Transistor consists of the following components as shown in Figure 2-8: lithographically defined gate electrodes which surround the silica nanotube, deep etched source-drain microfluidic channels, and PDMS (polydiemethylsiloxane) cover KCl solution is used as the nano-channel fluid [8, 9].

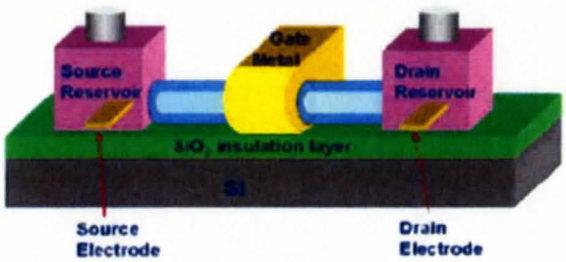

Figure 2-8 Schematic diagram of Nanofluidic FET, reprinted from ref. 8, 9

Voltages applied to the gate electrode shift the electrostatic potential distribution inside the nanotubes. In the case of silica nanotubes having negative surface charges, cations are the majority carriers so that negative V_g will enhance cation concentration while positive V_g depletes cations.

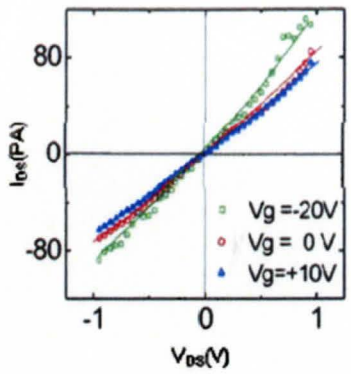

Figure 2-9 Drain current vs drain voltage at different values of gate voltage in Nanofluidic FET, reprinted from ref. 8, 9

2.3 Advantages of Field-Effect Transistors

2.3.1 Advantages of Inorganic Field-Effect Transistors

The continuous improvement of integrated circuit performance is a prerequisite for the success of the modern electronic industry This improvement is achieved by reducing the featured size of the fundamental switching component, MOSFETs, the most important type of the IFETs. Indeed, the reduction of device dimensions, or scaling, allows the packing of a great number of circuit functions into a small space. As a result complex electronic equipment can be employed in many applications where weight and space are critical, such as in aircrafts or space vehicles.

In addition, the large-scale integration of many IFETs based circuits on a Si substrate has led to a major reduction in computer size, thereby tremendously increasing speed and function density of the operating system. An example of this is the 45nm Intel SRAM chip which has more than 1 billion IFETs.

2.3.2 Advantages of Organic Field-Effect Transistors

Compared with conventional IFETs, the OFETs fabrication process is much less complex. This is due to the much lower temperature deposition and solution processing techniques that can be applied on a variety of substrates.

At the same time, mechanical flexibility of organic channel materials makes the relevant devices naturally compatible with plastic substrates for light weight and foldable products.

Another advantage of OFETs is their high portability, which leads to the miniaturization of devices. Small sample volumes as well as arrays with many elements are also achievable [41, 42].

2.3.3 Advantages of Micro/Nanofluidic Field-Effect Transistors

Micro/Nanofluidic Field-Effect Transistors have made great progress within the last decade and offer promising potentials in the future. The key to Micro/Nanofluidic FETs is the manipulation of fluids within micrometer or

nanometer-sized channels. In this case, micro-fabricating techniques adapted from the semiconductor and plastic industries such as micromachining, photolithography and injection moulding are applied in the micro/nanofluidic FETs industry. These achievable miniaturization methods bring the following benefits: reduction of the size of the equipment, fast analysis, a short reaction times, parallel operation for multiple analyses, and the possibility of portable devices. Specific to the field of Micro/Nanofluidic FETs is the advantage of the fast analysis with low sample and reagent volumes, leading to low waste levels and the unique physical consequences of mico/nanoscale fluid flow, and ultimately establishing "lap-on-a-chip" systems. [43-45]

2.4 Applications of Field-Effect Transistors

2.4.1 Applications of Inorganic Field-Effect Transistors

Since the scientists in Bell Laboratories invented the world's first transistor in 1947, IFETs have dominated the mainstream microelectronics industry. They are fundamental building blocks for basic analytical circuits, such as amplifiers, as well as the key elements for digital combination logic circuits. Moreover, IFETs are essential to the modern memory devices, integrated circuits, and microprocessors used in personal computers and laptops [41].

2.4.2 Applications of Organic Field-Effect Transistors

Since the first OFET was reported in 1986 [27], there has been great progress in both the materials performance and development of new fabrication techniques. OFETs have already been demonstrated in the applications of: electronic papers for displays [46-48], sensor devices for chemical vapour and humidity sensing [49,50], pentacene-based OFETs integrated circuits for Radio Frequency Identification Cards (RFIDs) [5,51].

2.4.3 Applications of Micro/Nanofluidic Field-Effect Transistors

In conventional micro/nanofluidic devices, analytical separations can be achieved by micro/nanofluidic FETs which apply the on-chip operations including chemical separations by chromatography or electrophoresis [52, 53]. In conjunction with fluid manipulation and chemical separation, detection of analysis via optical, electrochemical and metric methods is another important application [54-57]. Moreover, nucleic acid analysis [58, 59], protein analysis [57, 59] and cellular studies are proved applicable in micro/nanofluidic devices for bioanalytical applications [60, 61].

Besides the applications in conventional micro/nanofluidic devices, it has been reported that the current control in a microfluidic FET was achieved by electrowetting between competitive insulating/conducting fluidics [10]. It has also been demonstrated in Nanofluidic FETs that gate voltage can modulate the

concentration of ions and molecules in the channel and controls the ionic conductance [8, 9, 62].

2.5 Disadvantages of Field-Effect Transistors

2.5.1 Disadvantages of Inorganic Field-Effect Transistors

As mentioned before, the 45nm Intel SRAM chip has more than 1 billion transistors per 300mm silicon wafer. However, such high precision requires a facility with a photolithography set-up that requires a huge capital investment. For example, a state-of-the-art 300mm silicon integrated circuit fabrication facility costs approximately US$3 billion, to which only a few industrial leaders, such as Intel, are able to finance.

The most common type of IFETs is typically Silicon complementary metal oxide semiconductor FET (Si-CMOSFET). This device is single-crystalline with typical carrier mobility near 1000 $cm^2/V \cdot s$ at room temperature, which accounts for the high performance. However it must be built on a silicon wafer, which has a limited diameter of approximately 300mm with high price of about US$1000 per piece. The high cost and limited dimension make it incompatible with some electronic markets including large-area displays and low-end applications such as RFID tags and E-Papers.

2.5.2 Disadvantages of Organic Field-Effect Transistors

Because of the relatively low mobilities of organic semiconductor channel materials, OFETs cannot compete with the performance of IFETs based on single-crystal Si or Ge semiconductor which have charge carrier mobilities (μ) at least three orders of magnitude higher than OFETs. For this reason, OFETs are not appropriate for applications that require very high switching speeds [42].

In order to meet benchmarks for performance criteria, such as mobility and on/off ratio, active layer materials should ideally be easy to process and have long-term stability for device longevity. However, there is a delicate balance between the performance and the processability of the active layer component, which becomes another disadvantage in current OFET technology [41]. For example, the reported organics possessing good electronic characteristics such as pentacene, is insoluble and therefore difficult to process [63, 64].

2.5.3 Disadvantages of Micro/Nanofluidic Field-Effect Transistors

In micro/nanofluidic FETs, fused silica nanotubes were used which led to the enhancement of the electrophoretic separation efficiency, rather than the gate control of flows in integrated devices [7].

Moreover, the experiments were carried out in nanotubes covered with a thin, ion-conductive polymer film. The the thickness of the nanotube walls required a high gate voltage to obtain sufficiently high radial electric fields, the voltage magnitude of which is far too high for today's integrated circuits [6, 8, 9].

With micro/nanotube channels, device sizes have been reduced to much smaller dimensions compared to conventional nanofabrication, but in terms of integration, it is more difficult.

3 OBJECTIVES

As mentioned in Chapter 2, the relatively low mobilities of the charge carriers in the channel and the delicate balance between the performance and the processability became the limitations of OFET development. At the same time, higher gate voltage required for integrated circuits and capillary effect affecting the gate control were also found to be the drawbacks of the nanofluidic devices. Therefore, Liquid Organic Field-Effect Transisotrs (LOFETs) with potential advantages and applications listed below have attracted much attention.

Potential advantages of LOFETs

- Wide range of channel materials
- Low cost
- Simple structure, nanotube-free
- Easy to assemble

Potential applications of LOFETs

- Sensing in low concentration conditions
- Biochemical sequencing

As a result, the objectives of this thesis were shown as below,

- Observe if Electric-field effect exists in LOFETs

- Study Current-Voltage (I-V) behaviour in LOFET devices, via parameters of gate voltage, channel length and channel fluids
- Study structure of channel materials X-ray diffraction, in order to control device behaviours in atomic scale more precisely

4 EXPERIMENTAL PROCEDURE/DETAILS

4.1 LOFET Design and Construction

Schematics of LOFET design in both internal gate mode and external gate mode were shown in Figure 4- 1. The LOFET cell is composed of electrodes and solution container. The electrodes include source, drain and double-gate electrodes which are prepared from platinum foil. Pre-cleaned micro cover glasses (VWR, Ltd.) with designed sizes are assembled by instant glue (Elmer's Products Canada, Corporation) which cannot be dissolved in N,N-Dimethylformamide, the solvent of the channel materials. Therefore good electrical contact as well as a proper sealed organic solution is attained.

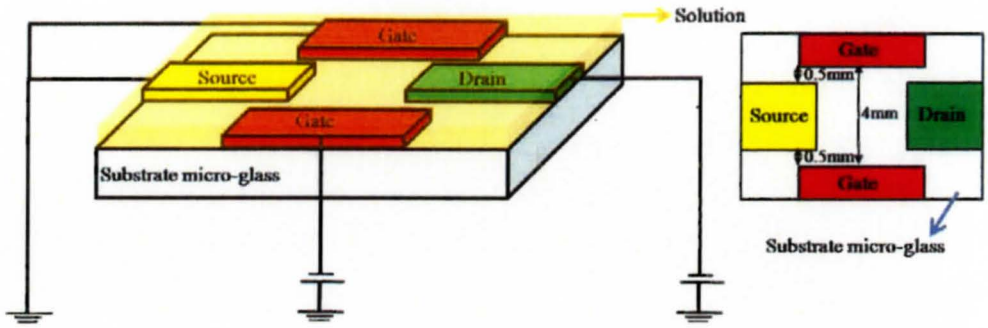

(a)

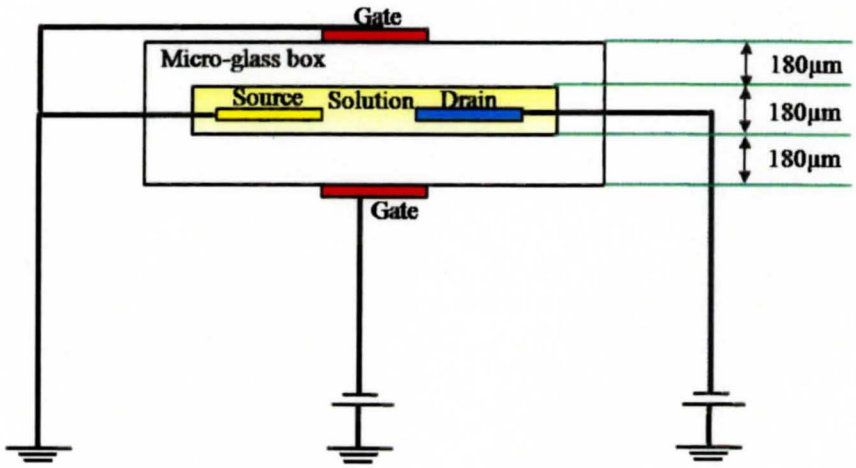

(b)

Figure 4- 1 Schematic diagrams of Liquid Organic Field-Effect Transistor (LOFET): (a) internal gate mode, (b) external gate mode

4.2 Preparations of electrodes and solution

Source, drain and double-gate electrodes are made from 99.99% pure platinum foil produced by Alfa Aesa. Before being placed into the LOFET cell, all the electrodes had been immersed in concentrated hydrochloric acid and subsequently heated up to 80°C for 2 hours in order to eliminate metal impurities. Deionized water was used to flush the electrodes. Acetone and N,N-Dimethylformamide were also used to clean the electrodes in order to keep the organic impurities away from the electrodes. In the final step, the electrodes were dried in vacuum overnight so that the influence from water vapour to the cell has been minimized.

N,N-Dimethylformamide (Caledon Laboratories Ltd.) was selected as the solvent of the channel fluid shown as Figure 4- 2. Small-molecule organic chemicals such as 4,4'-Dihydroxybiphenyl, 2-(4-Hydroxyphenyl)-5-pyrimidinol and 2-Amino-4 Phenylphenol were obtained from Sigma-Aldrich Canada and used as the solute of the channel fluid, structures of which are shown in Figure 4- 3.

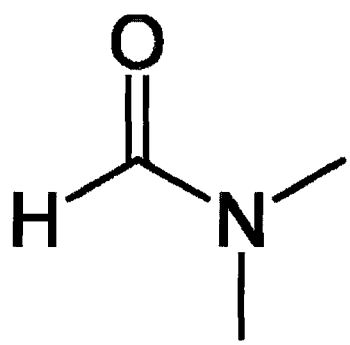

Figure 4- 2 Solvent structure of the channel fluid, N,N-Dimethylformamide

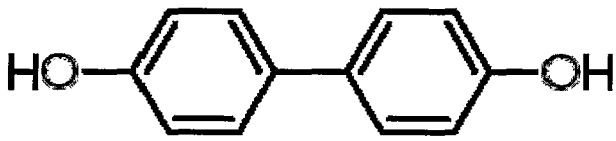

(a)

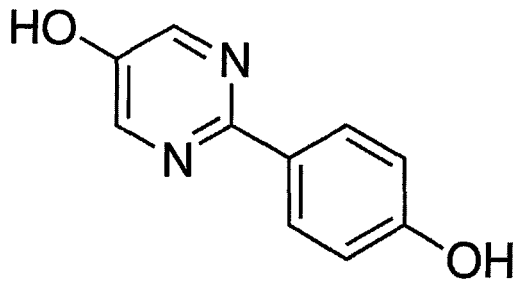

(b)

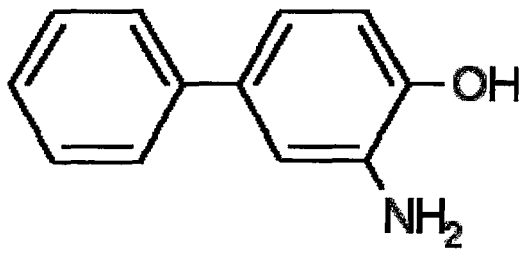

(c)

Figure 4- 3 Solute structures of the channel fluid: (a) 4,4'-Dihydroxybiphenyl, (b) 2-(4-Hydroxyphenyl)-5-pyrimidinol and (c) 2-Amino-4-Phenylphenol

4.3 Experimental Set-up and I-V Measurement

Figure 4-4 is the experimental apparatus for the LOFET cell operation and measurement. Source-drain and double-gate electrodes are all kept inside the cell,

perpendicular to each other The LOFET cell was placed in a Faraday shield which lowered the electronic noise effectively

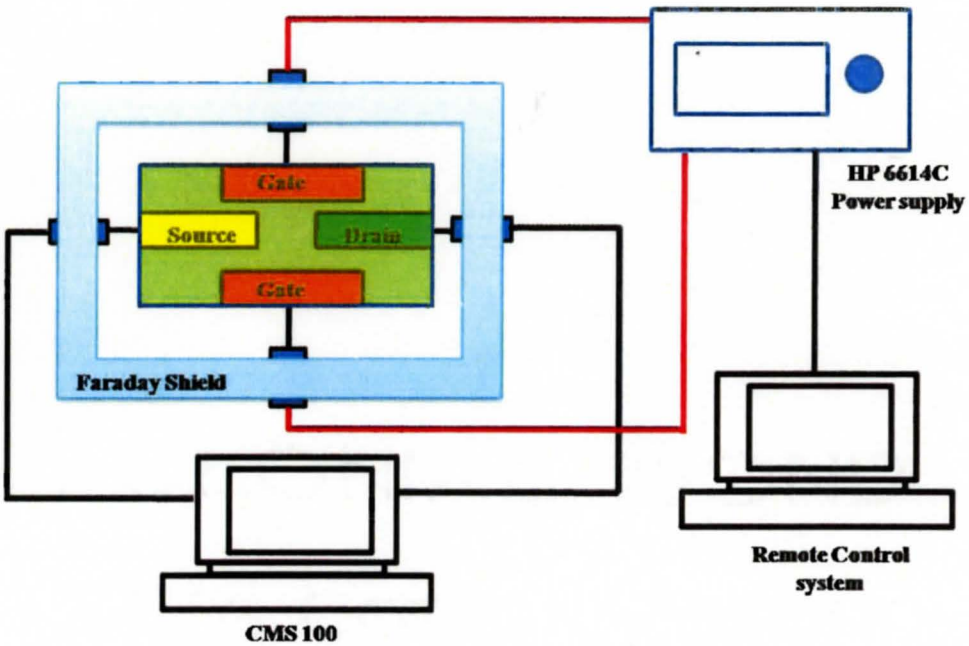

Figure 4-4 Schematic diagram of LOFET cell operation and measurement apparatus

The variable voltage for double-gate was controlled by Hewlett Packard DC Power Supply (Model 6614C), and gate current is recorded by Keithley Picoammeter (Model 485). The system is operated by programs written in Visual Basic Language as the experiment progressed. Gamry Instruments CMS 100 Electrochemical Analyzer and Framework Software System were used to record I-V Curves between source and drain electrodes. All the measurements were taken with samples kept in the shield at room temperature.

4.4 Visualization Techniques

4.4.1 Optical Microscope Observation

The Axioplan 2 Imaging and Axiohot 2 University Microscope were used for optical microscope observation of the electrode surface in order to obtain better understanding of the reason behind the phenomena.

4.4.2 X-Ray Diffraction Observation

The composition of the film formed in the channel was studied by XRD with a diffractometer (NicoletI2) using Cu Kα radiation at a scanning rate of 0.16°/min.

5 EXPERIMENTAL RESULTS AND DISCUSSION

LOFET were successfully fabricated by using the four-probe configuration. The experimental results were obtained in both internal gate mode and external gate mode. The influence of gate voltage, channel length and channel fluid type on the current-voltage behaviour of the devices was investigated.

5.1 Current-Voltage Behaviours of LOFETs in Internal Gate Mode

5.1.1 Impact of Gate Voltages

To study the effect of gate voltage to drain current in internal gate mode, 0.5mol/L of 2-(4-Hydroxyphenyl)-5-pyrimidinol channel fluid was prepared and a channel 2mm in length was made. The applied source-to-drain voltage was set within a range from 0V to 1V at a scan rate of 50mV/s. Figure 5- 1 shows the source-to-drain current for the gate voltage varying from 0 to 5V. As the magnitude of gate voltage increased, the current in the channel increased significantly. The main reason for the increase of the drain current is due to the increase of the anion concentration inside the channel of the LOFETs, which will be explained in details in the following sections.

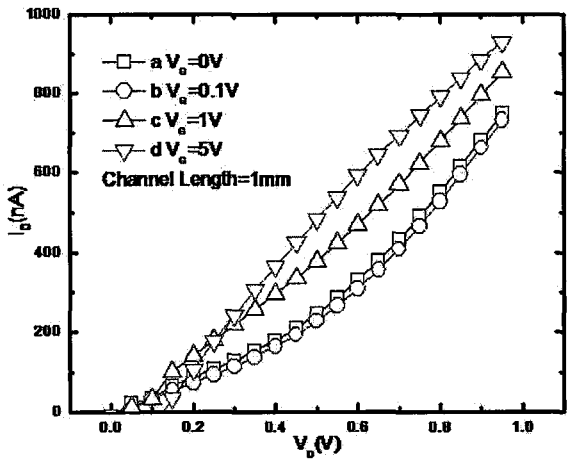

Figure 5- 1 Effect of gate voltage on drain current with respect to drain voltage in 0.5mol/L of 2-(4-Hydroxyphenyl)-5-pyrimidinol channel fluid with a channel length of 1mm: (a) V_G=0V, (b) V_G=0.1V, (c) V_G=1.0V, (d) V_G=5.0V

Inside the LOFET channel filled with 0.5mol/L of 2-(4-Hydroxyphenyl)-5-pyrimidinol fluid, there is equilibrium:

$$OH\text{-}R_1\text{-}R_2\text{-}OH \leftrightarrow {}^{-}O\text{-}R_1\text{-}R_2\text{-}OH + OH\text{-}R_1\text{-}R_2\text{-}O^{-} + {}^{-}O\text{-}R_1\text{-}R_2\text{-}O^{-} + H^{+}$$

The ionic current under source-to-drain voltage can be calculated as a superposition of conductive and convective contributions

$$I = \int_{-h}^{h} we[(n_+ + n_-)\mu E + (n_+ - n_-)u]dx \qquad (5.1.1)$$

Eq. (5.1.2) above is the integration over the volume of the channel, where w, $2h$, μ, $n+$ and $n-$ are the width, height of the channel, ionic mobility, cation and anion concentrations, respectively [65, 66].

To further understand the gate effect and determine the ions that dominate the drain current, protons that possess the highest mobility among all the particles in the channel fluid were assumed as the majority carriers. 0.05ml of hydrochloric acid with a pH value of 1.70 was added to 1ml of 0.5mol/L of 2-(4-Hydroxyphenyl)-5-pyrimidinol channel fluid. As a result, the pH value of the fluid decreased from 8.50 to 5.90. The drain current in the channel with proton additives was two times higher than it is in the pure fluid as shown in Figure 5- 2. At the same time, the proton concentration in the acid fluid was 30,000 times higher than it was in the pure fluid. These observations contradict the assumption made before. As a result, anions with much lower mobilities such as $^{-}O\text{-}R_1\text{-}R_2\text{-}OH$, $OH\text{-}R_1\text{-}R_2\text{-}O^{-}$ and $^{-}O\text{-}R_1\text{-}R_2\text{-}O^{-}$ were the majority carriers.

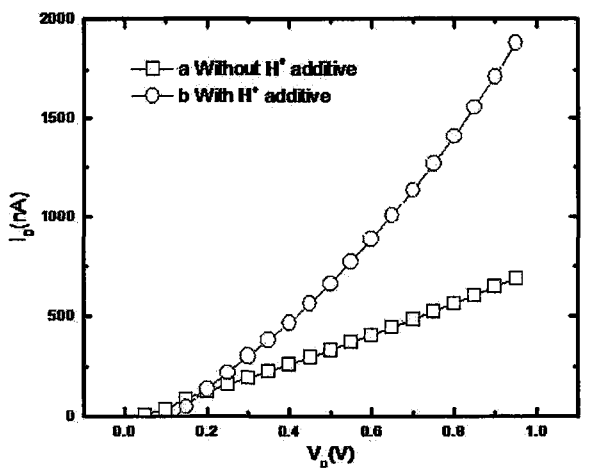

Figure 5- 2 Source-to-Drain current characteristics of 0.5mol/L of 2-(4-Hydroxyphenyl)-5-pyrimidinol solution with a channel length of 2mm and gate voltage of 1V: (a) without proton additive, (b) with proton additive

Anions became the majority carriers, resulting in an n-type Field-Effect Transistor (FET). Meanwhile the electrostatic potential distribution inside the channel varied under different positive voltages. Increasing gate voltage Vg enhanced anion concentration and thus resulted in larger drain current. This simple scheme explains quantitatively how electric-field works in LOFET systems. In semiconductor systems, the smaller the band gaps, the better the ambipolar behaviour. However, both cation and anion densities are associated with the same electrical potential level in fluidic channels. This phenomenon results in gapless transport systems.

It was reported that the following basic kinetic processes exist inside the nanofluidic channel: (i). deprotonation or protonation in response to the external electrical field, (ii) adsorption and desorption of counter ions, (iii) ion exchange in the channel leading to a steady state of ion distribution[8]. Experimental results in Figure 5- 3 showed that ionic conductance changed once gate voltage increased which are mainly due to reaction (i) or (ii). It decayed gradually to steady state under the same gate voltage, a high source-to-drain voltage sweeping led to a rapid decay (relaxation time < 50 sec at 5V) compared with the slower decay under lower voltage (relaxation time ~ 150 sec at 0.5V). However, it has also been observed that different gate voltages did not result in much different transient responses at the same source drain voltage in LOFETs. Therefore, ion-exchange between the transiently generated counter ions and bulk solution were believed to

control the kinetics of the field modulation in the liquid state channels in LOFETs. Further increasing the gate voltage should lead to faster field effect operation.

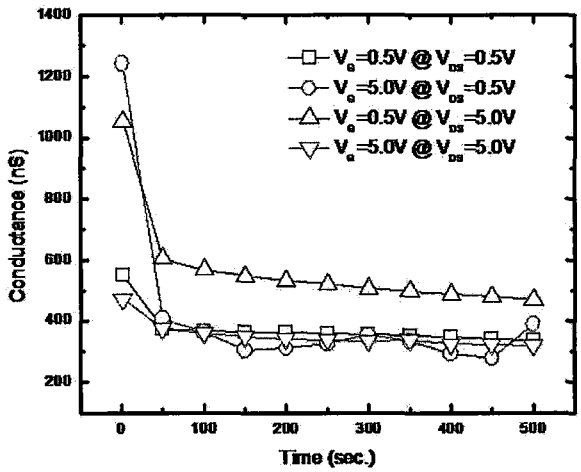

Figure 5- 3 The transient responses of ionic conductance when turning on the gate voltages, 0.5mol/L of 2-(4-Hydroxyphenyl)-5-pyrimidinol solution with a channel length of 2mm

Gate voltage effects were also obtained in a group of LOFETs filled with different small-molecule organic solutions inside the channels. The channel fluids are 4,4'-Dihydroxybiphenyl, 2-(4-Hydroxyphenyl)-5-pyrimidinol and 2-Amino-4-Phenylphenol solutions in a concentration of 0.5mol/L. These solutions were injected into 2mm channels one after another for the current-voltage behaviour measurement. From Figure 5- 4 to Figure 5- 6, it is obvious that drain current increased significantly while the gate voltage increased from 0V to 5V in all three LOFETs.

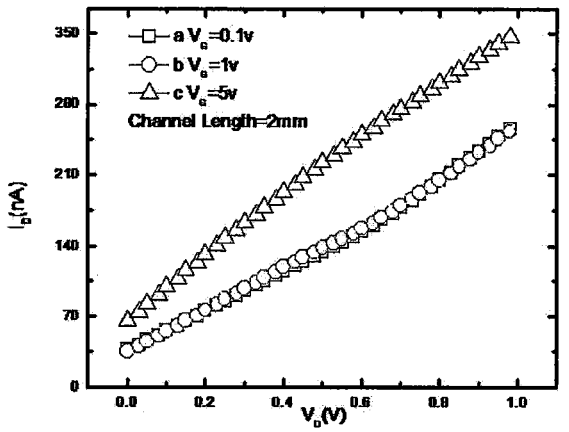

Figure 5- 4 Effect of gate voltage on drain current with respect to drain voltage in 0.5mol/L of 4,4'-Dihydroxybiphenyl solution with a channel length of 2mm: (a) V_G=0V, (b) V_G=1.0V, (c) V_G=5.0V

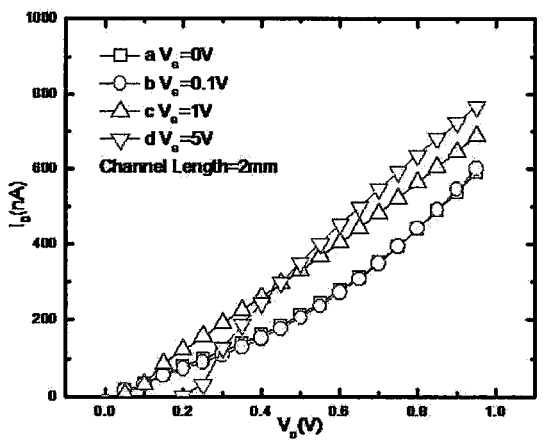

Figure 5- 5 Effect of gate voltage on drain current with respect to drain voltage in 0.5mol/L of 2-(4-Hydroxyphenyl)-5-pyrimidinol solution with a channel length of 2mm: (a) V_G=0V, (b) V_G=0.1V, (c) V_G=1.0V, (d) V_G=5.0V

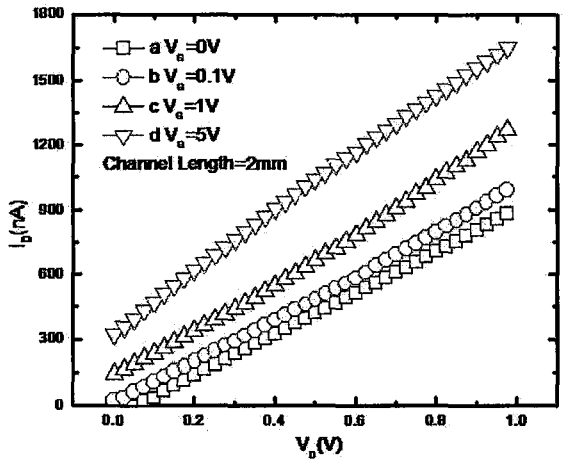

Figure 5- 6 Effect of gate voltage on drain current with respect to drain voltage in 0.5mol/L of 2-Amino-4-Phenylphenol solution with a channel length of 2mm: (a) V_G=0V, (b) V_G=0.1V, (c) V_G=1.0V, (d) V_G=5.0V

From the results above, a preliminary summary is given below:

1) The impact of gate voltage on source-to-drain current is significant. The drain current jumped up once the gate voltage increased. This phenomenon has been discovered in all LOFET specimens with different channel fluids and channel lengths.

2) Anions are the majority carriers in LOFETs of the four-probe internal gate mode. Anion concentration inside the channel increased while applying a larger voltage to the gate, resulting in the increase of the drain current.

5.1.2 Effect of Channel Length

The effects of channel lengths of LOFETs on the current-voltage behaviour are shown from Figure 5- 7 to Figure 5- 10. The drain current increased linearly when the source-to-drain voltage was increased from 0V to 1V. At the same time, the current decreased when the channel length was increased from 1mm to 4mm, and this coincided with the equation below for the linear regime in FETs:

$$I_D = \frac{Z\mu C_i}{L}(V_G - V_T)V_D \qquad (5.1.3)$$

It was discovered that at the same source-to-drain voltage, the difference between drain current in various channels increased notably when the gate voltage was increased from 0V to 5V. This is related to the change in anion concentration with varying gate voltages as mentioned in the previous section.

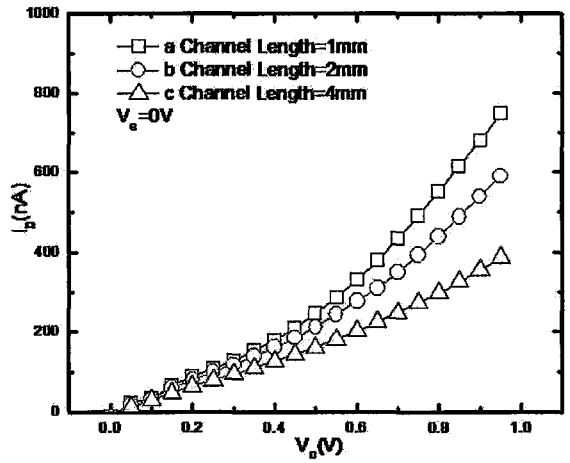

Figure 5- 7 Effect of channel length on drain current with respect to drain voltage in 0.5mol/L of 2-(4-Hydroxyphenyl)-5-pyrimidinol channel fluid with a gate voltage of 0V: (a) channel length=1mm, (b) channel length=2mm, (c) channel length=4mm

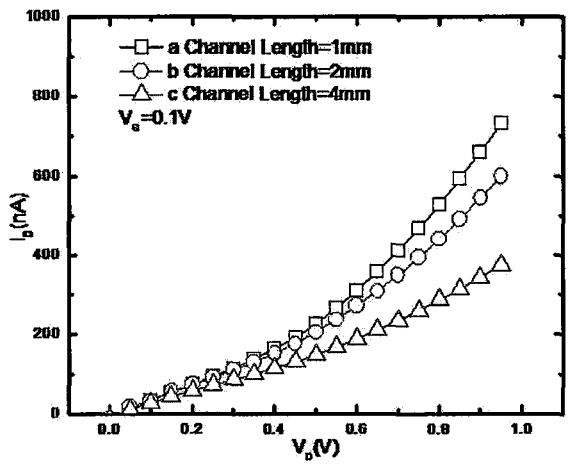

Figure 5- 8 Effect of channel length on drain current with respect to drain voltage in 0.5mol/L of 2-(4-Hydroxyphenyl)-5-pyrimidinol channel fluid with a gate voltage of 0.1V: (a) channel length=1mm, (b) channel length=2mm, (c) channel length=4mm

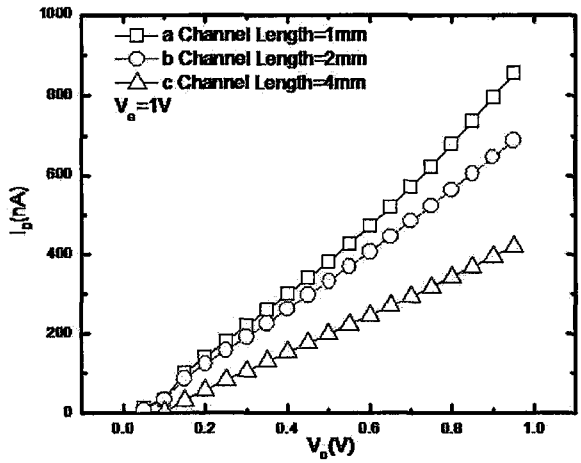

Figure 5- 9 Effect of channel length on drain current with respect to drain voltage in 0.5mol/L of 2-(4-Hydroxyphenyl)-5-pyrimidinol channel fluid with a gate voltage of 1V: (a) channel length=1mm, (b) channel length=2mm, (c) channel length=4mm

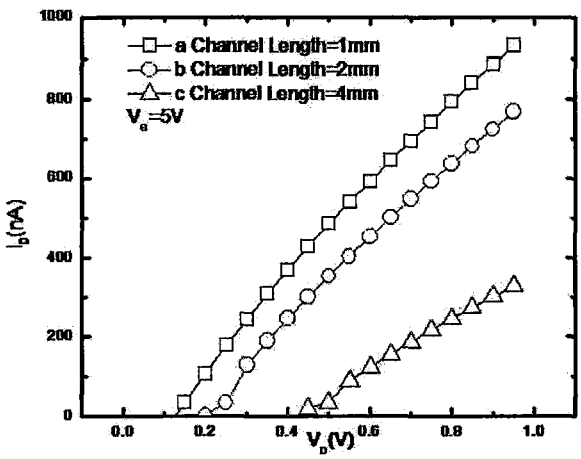

Figure 5- 10 Effect of channel length on drain current with respect to drain voltage in 0.5mol/L of 2-(4-Hydroxyphenyl)-5-pyrimidinol channel fluid with a gate voltage of 5V: (a) channel length=1mm, (b) channel length=2mm, (c) channel length=4mm

5.1.3 Discussion about Solute Structure of the Channel Fluid

The effects of solute structure and polarity on LOFET performance were also studied from Figure 5- 11 to Figure 5- 13. The drain currents of three different channel fluids were measured while the gate voltage increased from 0.1V to 5V.

It was found that when the polarity of the molecules increased from 4,4'-Dihydroxybiphenyl to 2-Amino-4 Phenylphenol, the drain current increased significantly. At the same time, the difference between drain current in specific solutions also increased when the gate voltage was increased from 0.1V to 5V. According to these results, the idea of molecule sequencing was generated by using this four-probe internal gate mode LOFET. It is possible that different types of channel fluids can be distinguished by their characteristic drain current. At the same time, more obvious results can be achieved by simply increasing the gate voltage.

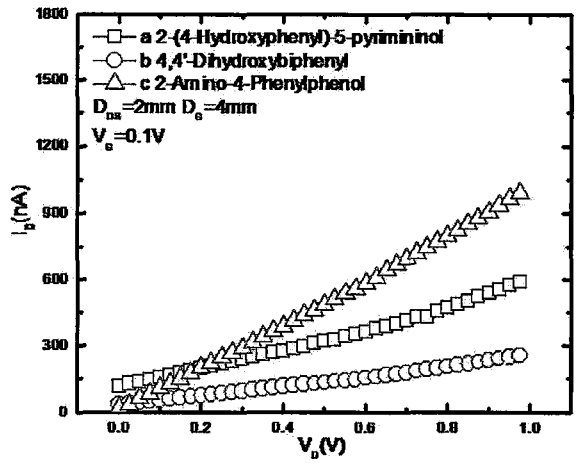

Figure 5- 11 Effect of solute structure on drain current with respect to drain voltage in 0.5mol/L of 2-(4-Hydroxyphenyl)-5-pyrimidinol channel fluid with a gate voltage of 0.1V: (a) 2-(4-Hydroxyphenyl)-5-pyrimininol, (b) 4,4'-Dihydroxybiphenyl, (c) 2-Amino-4-Phenylphenol

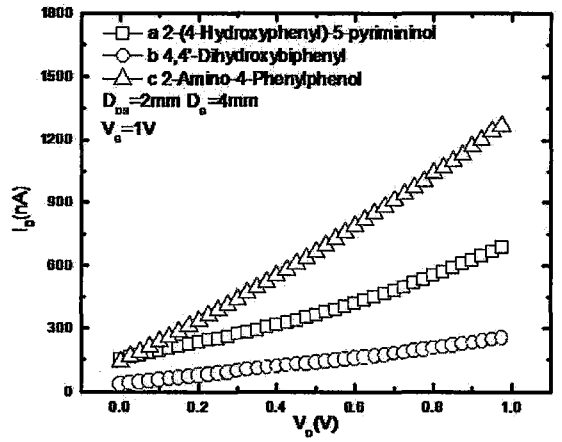

Figure 5- 12 Effect of solute structure on drain current with respect to drain voltage in 0.5mol/L of 2-(4-Hydroxyphenyl)-5-pyrimidinol channel fluid with a gate voltage of 1V: (a) 2-(4-Hydroxyphenyl)-5-pyrimininol, (b) 4,4'-Dihydroxybiphenyl, (c) 2-Amino-4-Phenylphenol

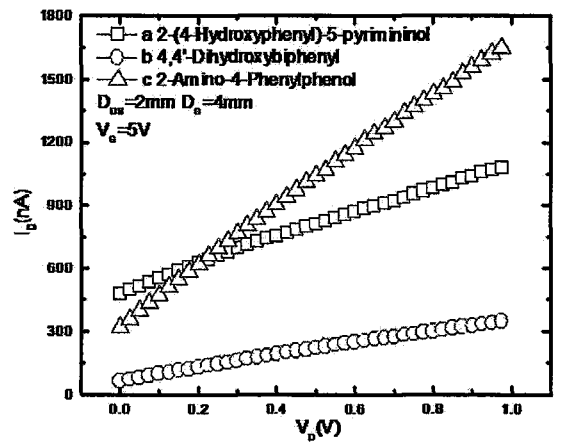

Figure 5- 13 Effect of solute structure on drain current with respect to drain voltage in 0.5mol/L of 2-(4-Hydroxyphenyl)-5-pyrimidinol channel fluid with a gate voltage of 5V: (a) 2-(4-Hydroxyphenyl)-5-pyrimininol, (b) 4,4'-Dihydroxybiphenyl, (c) 2-Amino-4-Phenylphenol

5.2 Current-Voltage Behaviours of LOFETs in External Gate Mode

5.2.1 Impact of Gate Voltages

To study the effect of gate voltage on drain current of LOFETs in internal gate mode, 1.063mol/L of 2-(4-Hydroxyphenyl)-5-pyrimidinol channel fluid was prepared and a channel 1mm in length was made. The applied source-to-drain voltage was set within the range from 0.45V to 0.50V. Figure 5- 14 shows the source-to-drain current for the gate voltage varying from 0 to 1500V. As the magnitude of gate voltage increased, the current in the channel decreased distinctively.

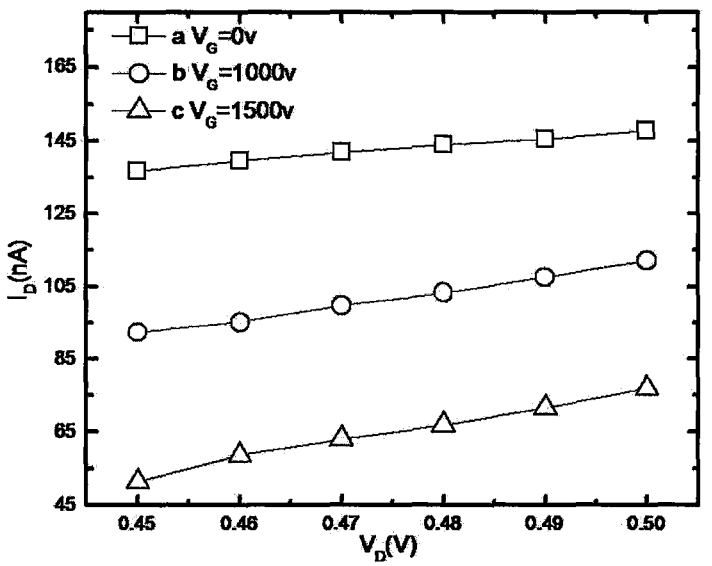

Figure 5- 14 Effect of gate voltage on drain current with respect to drain voltage in 1.063mol/L of 2-(4-Hydroxyphenyl)-5-pyrimidinol with a channel length of 1mm: (a) V_G=0, (b) V_G=1000V, (c) V_G=1500V

The gate voltage effect was obtained while the 1mm channel was filled with a higher concentration of 2.126 mol/L fluid as shown in Figure 5- 15. The drain current decreased notably when the gate voltage was increased from 0V to 1000V.

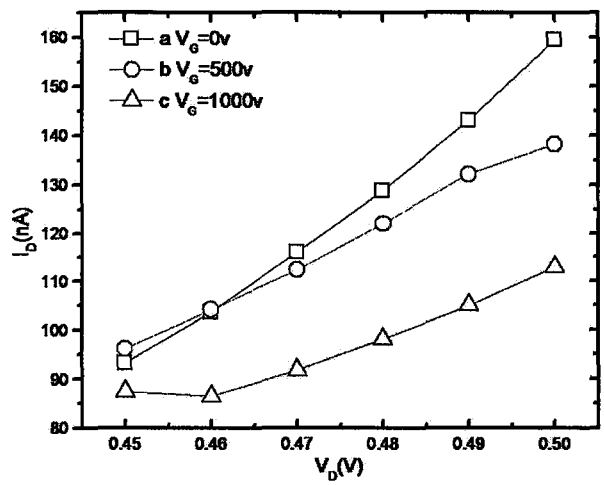

Figure 5- 15 Effect of gate voltage on drain current with respect to drain voltage in 2.126mol/L of 2-(4-Hydroxyphenyl)-5-pyrimidinol with a channel length of 1mm: (a) V_G=0, (b) V_G=1000V, (c) V_G=1500V

Applying different voltages to the external gate electrodes in the LOFETs with a 2mm channel, the drain current decreased once the magnitude of the gate voltage was enhanced. This phenomenon has been observed in both channels filled with 1.063mol/L and 2.126mol/L 2-(4-Hydroxyphenyl)-5-pyrimidinol fluid shown in Figure 5- 16 and Figure 5- 17, respectively.

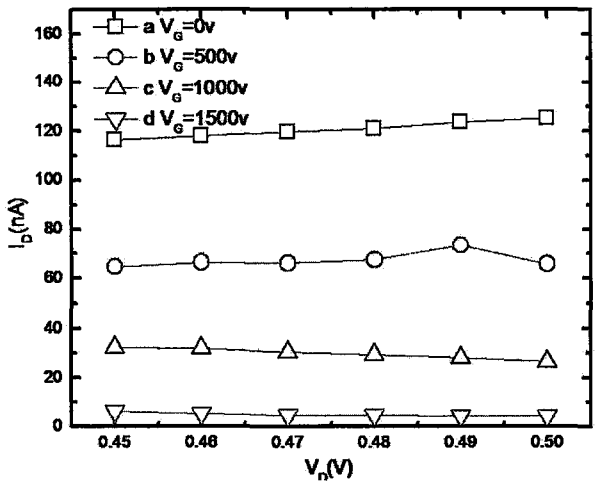

Figure 5- 16 Effect of gate voltage on drain current with respect to drain voltage in 1.063mol/L of 2-(4-Hydroxyphenyl)-5-pyrimidinol with a channel length of 2mm: (a) V_G=0, (b) V_G=500V, (c) V_G=1500V, (d) V_G=1500V

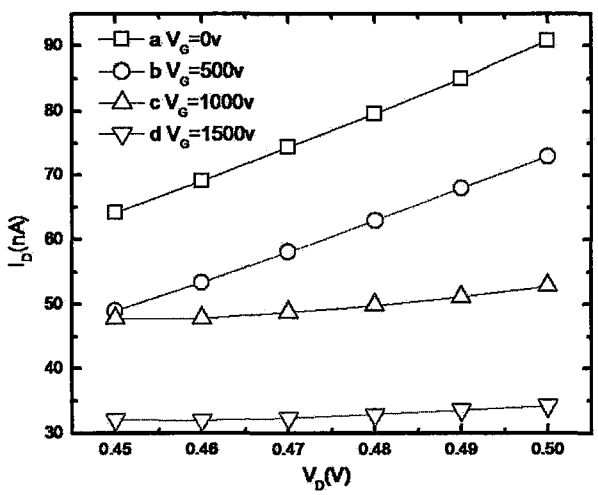

Figure 5- 17 Effect of gate voltage on drain current with respect to drain voltage in 2.126mol/L of 2-(4-Hydroxyphenyl)-5-pyrimidinol with a channel length of 2mm: (a) V_G=0, (b) V_G=500V, (c) V_G=1500V, (d) V_G=1500V

5.2.2 Effect of Channel Length

The effect of channel length on LOFET current-voltage behaviour in external gate mode was studied in 1.063mol/L of 2-(4-Hydroxyphenyl)-5-pyrimidinol channel fluid shown from Figure 5- 18 to Figure 5- 19. The drain current increased linearly when the source-to-drain voltage was increased from 0.45V to 0.5V. At the same time, the current decreased while the channel lengths increased from 1mm to 2mm, which coincided with the equation (5.1.3) for the linear regime in FETs:

It was discovered that at the same source-to-drain voltage, the difference between drain currents in 1mm and 2mm channels increased notably while the gate voltage increased from 0V to 1500V. And this is related to the change in anion concentration with varying gate voltage as mentioned in the previous section.

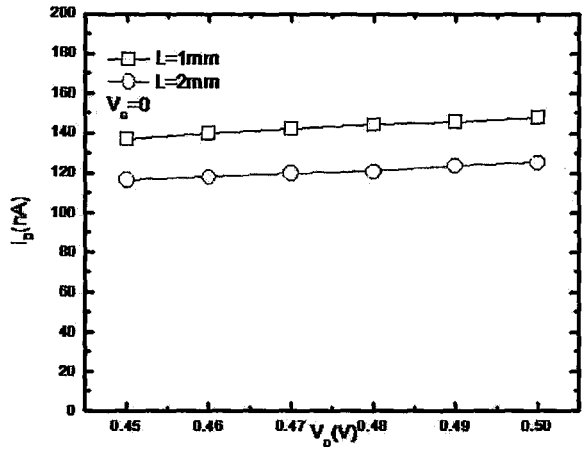
L=1mm
L=2mm
V_G=0
I_D(nA)
V_D(V)
200
180
160
140
120
100
80
60
40
20
0
0.45
0.46
0.47
0.48
0.49
0.50

(a)

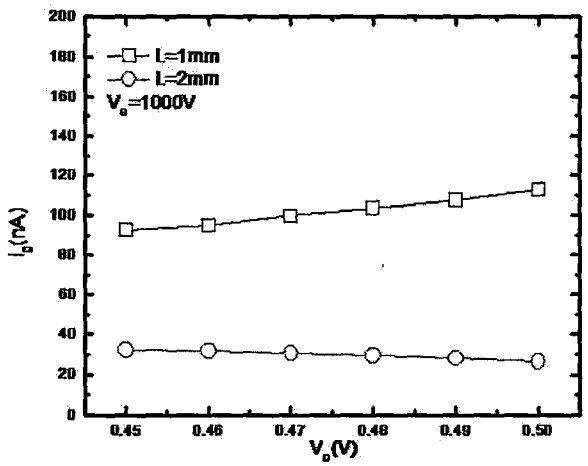
L=1mm
L=2mm
V_G=1000V
I_D(nA)
V_D(V)
200
180
160
140
120
100
80
60
40
20
0
0.45
0.46
0.47
0.48
0.49
0.50

(b)

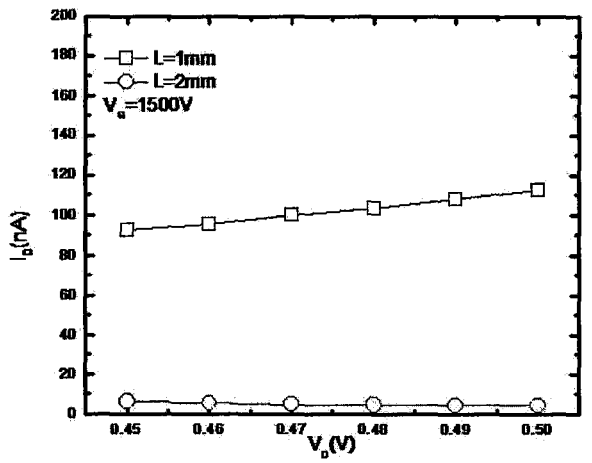

(c)

Figure 5- 18 Effect of channel length on drain current with respect to drain voltage in 1.063mol/L of 2-(4-Hydroxyphenyl)-5-pyrimidinol with channel lengths of 1mm and 2mm respectively: (a) V_G=0, (b) V_G=1000V, (c) V_G=1500V

While the concentration of the channel fluid increased to 2.126mol/L, the impact of the channel length on source-to-drain current was still significant. The drain current increased linearly when the source-to-drain voltage was increased from 0.45V to 0.5V. At the same time, the current decreased when the channel length was increased from 1mm to 2mm. It was found that at the same source-to-drain voltage, the difference between drain current from 1mm to 2mm channel length was larger in 500Vgate voltage than it was in 0V gate voltage.

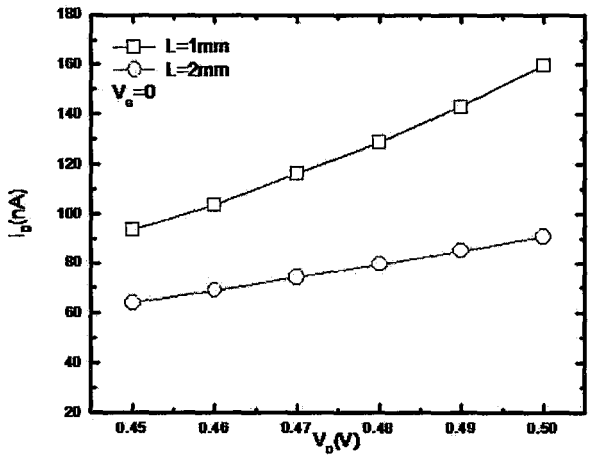

(a)

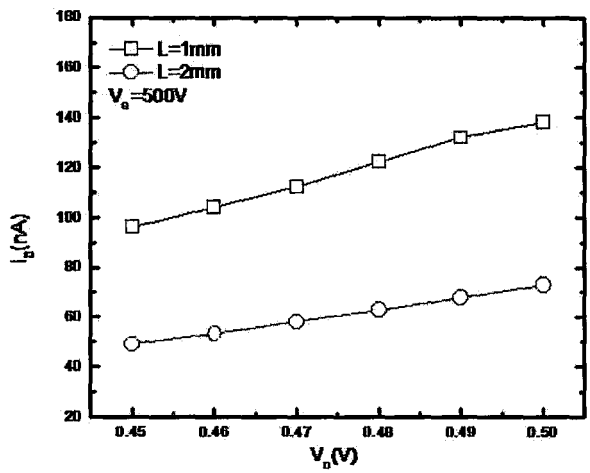

(b)

Figure 5- 19 Effect of channel length on drain current with respect to drain voltage in 2.126mol/L of 2-(4-Hydroxyphenyl)-5-pyrimidinol with channel lengths of 1mm and 2mm respectively: (a) V_G=0, (b) V_G=500V

5.2.3 Discussion about Channel Fluid Concentration

The effect of channel fluid concentration on LOFET current-voltage behaviour in external gate mode was compared between 1.063mol/L and 2.126mol/L of 2-(4-Hydroxyphenyl)-5-pyrimidinol. Such contrast in both 0V gate voltage and 1000V gate voltage were shown in Figure 5- 20 and Figure 5- 21, respectively. It is clear that the drain current of high-concentration channel fluid was always increasing more quickly than it was in low-concentration channel fluid.

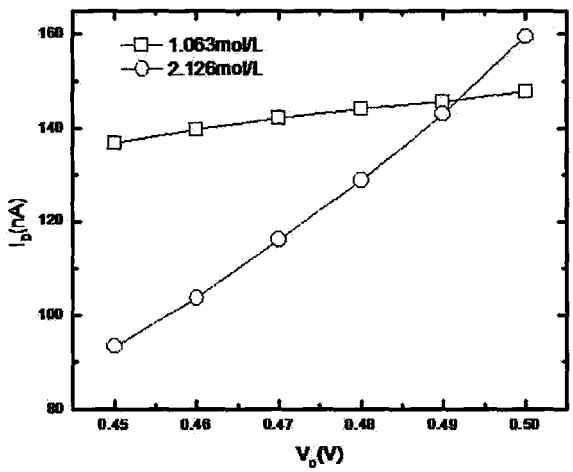

Figure 5- 20 Effect of channel fluid concentration on drain current with respect to drain voltage under V_G=0

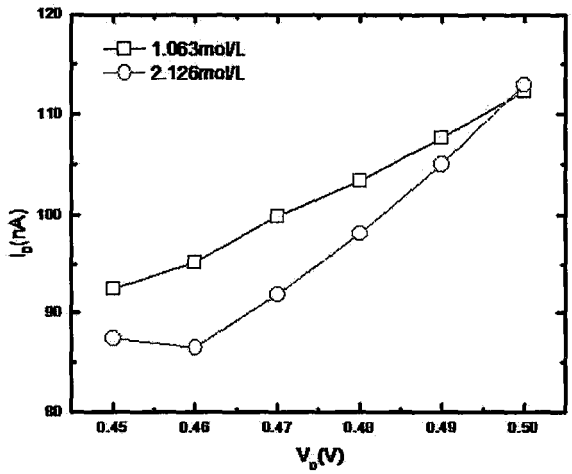

Figure 5- 21 Effect of channel fluid concentration on drain current with respect to drain voltage when V_G=1000V

6 CONCLUSIONS

In this thesis, different types of LOFETs in both internal gate mode and external gate mode were successfully fabricated by using four-probe configuration. Impact factors of the current-voltage behaviour of the device, such as gate voltage, channel length as well as channel fluid, were systematically studied.

It was discovered that varying gate voltage influenced source-to-drain current of LOFETs obviously in both internal and external gate modes. The drain current of internal gate mode increased significantly once the gate voltage was increased. This phenomenon has been found in all LOFETs samples of different channel fluids and channel lengths. It was also proven that anions including $^{-}O\text{-}R_1\text{-}R_2\text{-}OH$, $OH\text{-}R_1\text{-}R_2\text{-}O^{-}$ and $^{-}O\text{-}R_1\text{-}R_2\text{-}O^{-}$ were the majority carriers in LOFETs. The concentration of anions inside the channel increased when a larger voltage was applied to the gate, resulting in the increase of the drain current. This achievable gate modulation formed a good foundation for the research on the manipulation of ionic and molecular species.

It was also obtained that the drain current was changed when channel length was changed in two gate modes that were mentioned above. The current through the LOFET channel decreased when the magnitude of the channel length was increased: At the same time, the difference between drain currents in various channels increased significantly when the gate voltage was increased from 0V to

5V. This was found to be due to the anion concentration change with various gate voltages.

The drain current was also measured when LOFET channels were filled with fluids of different polarities. It is observed that with the polarity of the molecule increasing from 4,4'-Dihydroxybiphenyl to 2-Amino-4 Phenylphenol, the drain current increased significantly. At the same time, the difference between drain current in specific solutions were also more significant when applying a higher voltage to the gate. By combining these results with the gate modulation in LOFET channel fluid, there is of great potentials in developing new sensing techniques and even logic operation in the future.

LOFET research in this thesis represented a step towards new groups of ecnomic and efficient electronic component. Followed by systemic observations on the effects of gate voltage, channel length and channel fluid. It is obvious that LOFET will became a more attractive research topic because of its promising advantages in the future, such as easy fabrication, low cost and quickly sensitive response.

7 FURTHER WORK

The current-voltage behaviour was also measured inside the LOFET channel filled with conjugated polymer-based fluid. Poly(3,3'''-didodecylquarter-thiophene), PQT-12, which is widely used in advanced organic photon-electronic materials research, was chosen as the solute of the LOFET channel fluid. The structure of the film deposited on top of the electrode contact was studied by XRD. The data in zero magnitude gate voltage was compared with it was in 40V gate voltage. The peak appeared at a 2θ of 5° coincided with the PQT-12 reference patterns. It is clear that a diffraction peak appeared at a 2θ of 7.5° after applying a gate voltage of 40V to the device. It could be related to crystal orientation change caused by the increase of system energy, which was a result of the electric field effect.

However, the background noise from the current XRD facility is too high for further characterization on the film structure. High intensity and highly collimated beam techniques such as Synchrotron XRD is required for the future work on the gate effect of the LOFETs on crystal orientations as well as the texture changes in order to control the performance of the LOFET device more precisely.

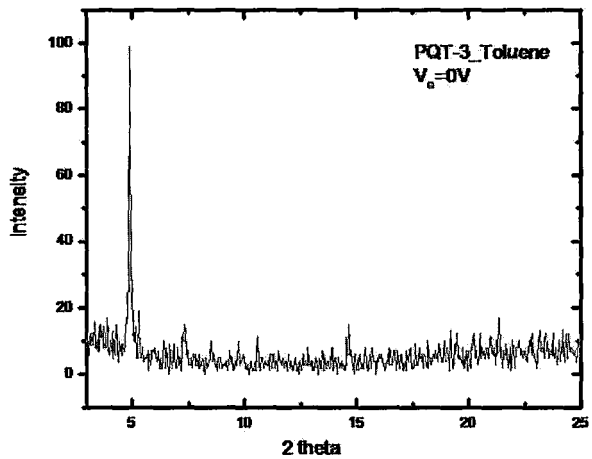

Figure 7- 1 XRD spectrum of the film deposited on top of the electrode without gate voltage

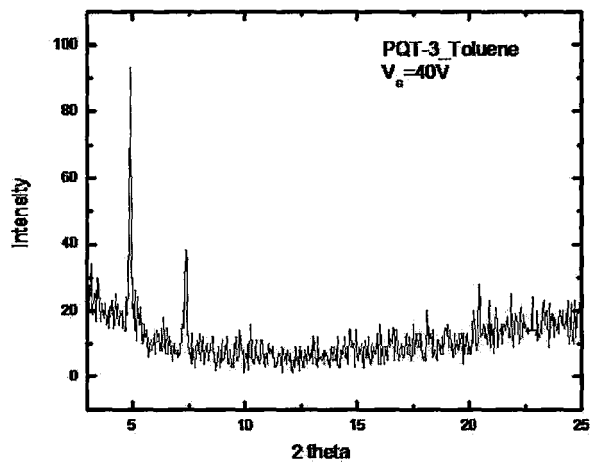

Figure 7- 2 XRD spectrum of the film deposited on top of the electrode with gate voltage of 40V

8 REFERENCE

1. J. J. Liou, F. Schwierz, *"RF MOSFET: recent advances, current status and future trends"*, Solid-State Electronics, 47 (2003), p1881–1895

2. M. J. Deen, F. Pascal, *"Electrical characterization of semiconductor materials and devices—review"*, Mater. Electron., 17(2006) p549–575

3. C. Di, G. Yu, Y. Liu, and D. Zhu, *"High-Performance Organic Field-Effect Transistors: Molecular Design, Device Fabrication and Physical Properties"*, J. Phys. Chem. B 111 (2007), p14083-14096

4. C. D. Dmitrakopoulos, D. J. Mascaro, *"Organic thin-film transistors: A review of recent advances"*, IBM J. RES. & DEV., VOL. 45 NO. 1 (2001), p11-27

5. D. Voss, *"Cheap and cheerful circuits"*, Nature, 407 (2000), p442-444

6. Paula Gould, "Mirofluidics realizes potential", Materials Today, July/August (2004), p48-52

7. R. B.M. Schasfoort, S. Schlautmann, J. Hendrikse, A. van den Berg, *"Field-Effect Flow Control for Microfabricated Fluidic Networks"*, Science, 286 (1999), p942-945

8. Rong Fan, Min Yue, Rohit Karnik, Arun Majumdar, and Peidong Yang, *"Polarity Switching and Transient Responses in Single Nanotube Nanofluidic Transistors"*, Physical Review Letters, 95 (2005), 086607 (4)

9. Rohit Karnik, Rong Fan, Min Yue, Deyu Li, Peidong Yang, and Arun Majumdar, *"Electrostatic Control of Ions and Molecules in Nanofluidic Transistors"*, NanoLetters, Vol. 5 (2005), No.5, p943-948

10. D. Y. Kim and A. J. Steckl, "Liquid-state field-effect transistors using electrowetting", Applied Physics Letters, (2007) 90, 043507

11. Lilienfeld, J. E. *"Method and apparatus for controlling electric currents,"* U. S. Patent No. 1,745,175 (Filed October 8, 1926. Issued January 18, 1930).

12. Lilienfeld, J. E. "Device for controlling electric current," U. S. Patent No. 1,900,018 (Filed March 28, 1928. Issued March 7, 1933).

13. Ben G. Streetman, Sanjay Kumar Banerjee, *"Solid State Electronic Devices"*, Pearson Education, 2006, p239-240

14. Brattain, Walter, "Bell Labs logbook", (December 1947), pp. 7–8, 24.

15. John Bardeen and Walter Brattain, *"The Transistor, a Semi-Conductor Triode,"* Physical Review 74 (15 July 1948) pp. 230–231

16. Bardeen J. and Brattain W., *"Three-Electrode Circuit Element Utilizing Semiconductor Materials"*, U.S. Patent 2524035, Filed June 17, 1948, issued Oct. 3, 1950

17. Becker J. A., and Shive, J. N., *"The Transistor – A New Semiconductor Amplifier"*, Electrical Engineering Vol. 68 (March 1949) pp. 215-221

18. Kahng, Dawon, *"Electric Field Controlled Semiconductor Device"*, U. S. Patent No. 3102230, Filed 31 May 31, 1960, issued August 27, 1963

19. Kahng, Dawon. *"Silicon-silicon dioxide field induced surface devices"*, Technical memorandum issued by Bell Labs (January 16, 1961) reprinted in Sze, S.M. Semiconductor Devices: Pioneering Papers. (Singapore: World Scientific Publishing Co., 1991) pp. 583-596.

20. Sah, C. T.,*"A new semiconductor triode, the surface-potential controlled transistor"*, Proceedings of the IRE, Vol. 49, No.11 (November 1961) pp. 1623-1634.

21. Hofstein, S.R. and Heiman, F.P., *"The Silicon Insulated Gate Field Effect Transistor"*, Proceedings of the IEEE, Vol. 51 (September 1963) pp. 1190 -1202.

22. D.D. Eley, *"Phthalocyanines as Semiconductors"*, Nature 1948, 162, p819

23. M. Pope, H.P. Kallmann, and P. Magnante, *"Electroluminescence in Organic Crystals"*, J. Chem. Phys. 1963, 38, p2042-2043

24. W. Helfrich, W.G. Schneider, *"Recombination Radiation in Anthracene Crystals"*, Phys. Rev. Lett. 1965, 14, p229-231

25. D. Kearns, M. Calvin, *"Photovoltaic Effect and Photoconductivity in Laminated Organic Systems"*, J. Chem. Phys. 1958, 29, p950-951

26. A. K. Ghosh, T. Feng, *"Merocyanine Organic Solar Cells"*, J. Appl. Phys. 1978, 49, p5982-5989

27. A.Tsumura, H. Koezuka, and T. Ando, *"Macromolecular electronic device: Field-Effect Transistor with a Polythiophene Film"*, Appl. Phys. Lett. 1986, 49(18), p1210-1212

28. Gilles Horowitz, *"Organic Thin Film Transistors: From theory to real devices"*, J. Mater. R., Vol. 19, No.7, Jul 2004, p1946-1962

29. G. Hadziioannou and G.G. Malliaras, *"Semiconducting polymers, Chemistry, Physics, and Engineering"*, Vol.2, p531-532

30. Christopher R. Newman, C. Daniel Frisbie, Demetrio A. da Silva Filho, Jean-luc Brédas, Paul C. Ewbank, and Kent R. Mann, *"Introduction to Organic Thin Film Transistors and Design of n-Channel Organic Semiconductors"*, Chem. Mater. 2004, 16, p4436-4451

31. Christos D. Dimitrakopoulos and Patrick R. L. Malenfant, *"Organic Thin Film Transistors for Large Area Electronics"*, Advanced Materials, 2002, 14, No.2, January 16, p99-117

32. Ziaie, B., *"Hard and soft micromachining for BioMEMS: review of techniques and examples of applications in microfluidics and drug delivery"*, Adv. Drug Delivery Rev., (2004) 56 (2), p145-172

33. Whitesides, G.M., *"SOFT LITHOGRAPHY IN BIOLOGY AND BIOCHEMISTRY"*, Annul. Rev. Biomed. Eng., (2001)3, p335-373

34. Quake, S. R. and Scherer, A., *"From Micro- to Nanofabrication with Soft Materials"*, Science, (2000) 290, p1536-1540

35. Berhard H. Weigl, Ron L. Bardell, Catherine R. Cabrera, *"Lab-on-a-chip for drug development"*, Advanced Drug Delivery Reviews, 55(2003), p349-377

36. L.J. Kricka, *"Microchips, microarrays, biochips and nano-chips: personal laboratories for the 21st century"*, Clin. Chim. Acta 307(1-2) (2001)

37. C.T. Crowe, D.F. Elger, J.A. Roberson, *"Engineering Fluid Mechanics"*, 7th Edition, John Wiley and Sons, 2000

38. Reynolds, *"An experimental investigation of the circumstances which determine whether the motion of water in parallel channels shall be direct*

or sinuous and of the flow of resistance in parallel channels", Phil. Trans. Roy. Soc. 174(1883), p935-982

39. T B Jones, "An electromechanical interpretation of electrowetting", Journal of Micromechanics and Microengineering, 15 (2005), p1184-1187

40. Frieder Mugele and Jean-Christophe Baret, "Electrowetting: from basics to applications", Journal of Physics Condensed Matter, 17(2005), pR705-R774

41. Colin Reese, Mark Robert, Mang-mang Ling, and Zhenan Bao, *"Organic Thin Film Transistors"*, Materials Today, September (2004), p20-27

42. Jason Locklin, Zhenan Bao, *"Effect of morphology on organic thin film transistor sensors"*, Anal. Bioanal. Chem., 384 (2006), p336-342

43. Gina S. Fiorini and Daniel T. Chiu, *"Disposable microfluidic devices: fabrication, function, and application"*, Biotechniques,38 (2005), p429-446

44. Rohit Kamik and Kenneth Castelino, *"Field-effect control of protein transport in a nanofluidic transistor circuit"*, 88 (2006), p123114-(1-3)

45. Stephen R. Quake and Axel Scherer, *"From Micro- to Nanofabrication with Soft Materials"*, Science, 290(2000), p1536-1540

46. J. A. Rogers, Z. Bao, K. Baldwin, A. Dodabalapur, B. Crone, V. R. Raju, V. Kuck, H. Katz, K. Amundson, J. Ewing, and P. Drzaic, *"Paper-like electronics displays: Large-area rubber-stamped plastic sheets of electronics and microencapsulated electrophoretic inks"*, Applied Physical Science, 98 (2001), p4835-4840

47. G. H. Gelinck, H. E. Huiteima, E. V. Veenendaal, E. Cantatore, L. Schrijnemakers, J. B. P. H. Van Der Putten, T. C. T. Geuns, M. Beenhakkers, J. B. Giesbers, B. Huisman, E. J. Meijer, E. M. Benito, F. J. Touwslager, A. W. Marsman, B. J. E. Van Rens and D. M. De Leeuw, *"Flexible active-matrix isplays and shift registers based on solution-processed organic transistors"*, Nature Materials, 3 (2004), p106-110

48. C. D. Sheraw, L. Zhou, J. R. Huang, D. J. Gundlach, T. N. Jackson, M.G. Kane, I. G. Hill, M. S. Hammond, J. Campi, B. K. Greening, J. Francl and J. West, *"Organic thin-film transistor-driven polymer-dispersed liquid crystal display on flexible polymeric substrates"*, Applied Physical Letters, 80 (2002), p1088-1090

49. Z. Zhu, J. T. Mason, R. Dieckmann, and G. G. Malliaras, *"Humidity sensors based on pentacene thin-film transistors"*, 81 (2002), p4643-4645

50. B. K. Crone, A. Dodabalapur, R. Sarprdhkar, A. Gelperin, H. E. Katz and Z. Bao, *"Organic oscillator and adaptive amplifier circuits for chemical vapour sensing"*, Journal of Applied Physics, 91 (2002), p10140-10146

51. P. F. Baude, D. A. Ender, M. A. Haase, T. W. Kelly, D. V. Muyres, S. D. Theiss, *"Pentacene-based radio-frequency identification circuitry"*, Applied Physics Letters, 82 (2003), p3964-3966

52. D. J. Harrison, A. Manz, Z. Fan, H. Luedi, and H. M. Widmer, *"Capillary electrophoresis and sample injection systems integrated on a planar glass chip"*, Analytical Chemistry, 64 (1992), p1926-1932

53. A. Manz, Y. Miyahara, J. Miura, Y. Watanabe, H. Miyagi, and K. Sato, *"Design of an open-tubular column liquid chromatography using silicon chip technology"*, Sens. Actuators B, B1 (1990), p249-255

54. M. A. Schwarz, and P. C. Hauser, *"Recent developments in detection methods for microfluidic channels"*, Lab Chip, 1 (2001), p1-6

55. N. A. Lacher, K. E. Garrison, R. S. Martin, and S. M. Lunte, *"Microchip capillary electrophoresis/electrochemistry"*, Electrophoresis, 22 (2001), p2526-2536

56. J. Wang, *"Electrochemical detection for microscale analytical systems: a review"*, Talanta, 56 (2002), p223-231

57. N. Lion, T. C. Rohner, L. Dayon, I. L. Arnaud, E. Damoc, N. Youhnovski, Z. Y. Wu, C. Roussel, "Microdulidc systems in protemics", Electrophoresis, 24 (2003), p3533-3562

58. J. P. Lauders, "Molecular diagnostics on electrophoretic microchips", Analytical Chemistry, 75 (2003), p2919-2927

59. E. Verpoorte, *"Microfluidic chips for clinical and forensic analysis"*, Electrophoresis, 23 (2002), p677-712

60. G. M. Whitesides, E. Ostuni, S. Takayama, X. Y. Jiang, and D. E. Ingber, "Soft lithography in biology and biochemistry", Annual Review of Biomedical Engineering, 3 (2001), p335-373

61. H. Andersson and A. van den Berg, "Microfluidic devices for cellomics: a review", Sens. Actuators B, 92 (2003), p315-325

62. Hirofumi Daiguji, Peidong Yang, and Arun Majumdar, "Ion Transport in Nanofluidic Channels", Nanoletters, 4(2004), p137-142

63. Y. Lin; D.I Gundlach; S.F Nelson; and T.N Jackson, *"Pentacene-Based Organic Thin-Film Transistors"*, 44 (1997), p1325-1331

64. O. D. Jurchescu, J. Baas, and T. T. M. Palstraa, *"Effect of impurities on the mobility of single crystal pentacene"*, 84 (2004), p3061-3063

65. S. Levine, J. R. Marriott, K. Robinson, *"Theory of Eletrokinetic Flow in a Narrow Parallel-Plate Channel"*, 71 (1975), p1-11

66. J. Israelachvili, *"Intermolecular and surface forces"*, 2nd edition, Academic Press: London, 2003